



# Sea-effect snowfall in the Baltic Sea area in 1998–2018 derived from convection-permitting climate model data

Meri Virman<sup>1</sup>, Taru Olsson<sup>1</sup>, Petter Lind<sup>2</sup>, and Kirsti Jylhä<sup>1</sup>

<sup>1</sup>Finnish Meteorological Institute, Helsinki, Finland

<sup>2</sup>Rosby Centre, Swedish Meteorological and Hydrological Institute, Norrköping, Sweden

**Correspondence:** Meri Virman (meri.virman@fmi.fi)

**Abstract.** Sea-effect snowfall forms frequently over the Baltic Sea in northern Europe. In its bordering countries, large snow accumulations and poor visibility associated with these, often intense, convective snowbands have had considerable impacts on society. This study presents, for the first time, the occurrence of snowband days over the full Baltic Sea area on climatological time scales. The climatology is investigated using a 21-year simulation made with the HARMONIE-Climate convection-permitting regional climate model applied at 3 km resolution. Snowband days occur most frequently (up to a few days per year in a 3 km × 3 km area) over specific regions of the Baltic Sea: near the eastern coast of Sweden, over the Gulf of Finland and the Northern Baltic Proper. Over majority of the northern Baltic Sea, snowbands occur typically between November–February. Winds with an easterly component favour the occurrence of snowbands along the eastern coast of Sweden and southern coast of Finland, whereas few cases in those regions occur with westerly winds. In addition, snowband days occur over the southern Baltic Sea, where the formation of snowbands is favoured by low-level winds having a northerly component and typically between December–March. This study supports operational forecasting of snowbands events and forms the basis for future research on how the occurrence of these events may change in a changing climate.

## 1 Introduction

Sea-effect snowfall (also commonly referred to as lake-effect snowfall) is convective precipitation that can form over relatively warm and ice-free water surfaces (e.g. lakes and seas) when the airmass above is cold enough. Sea-effect snowfall systems can take many shapes and sizes, but they typically occur as elongated and narrow snowbands leading to localized snowfall (Fig. 1). Under suitable wind conditions, the systems may drift from the sea to land, where snowbands can cause significant societal and economic impacts along the coastline, such as damage to infrastructure due to snow load, traffic disruptions due to poor visibility and excess snow on roads.

Lake-effect snowfall is notorious especially in the Great Lakes region in North America (see e.g., Hjelmfelt and Braham, 1983), where it has been studied extensively. Considerable snowfall amounts caused by the sea-effect have been documented in the Baltic Sea region (Rutgersson et al., 2022), such as in Finland (Olsson et al., 2017, 2018; Juga, 2010; Juga et al., 2014; Niemelä, 2012; Mazon et al., 2015, and Olsson et al., 2020, 2022, from hereon referred to as OLS2020 and OLS2022), Sweden (Jeworrek et al., 2017, from hereon referred to as JEW2017) and Poland (Bednorz et al., 2022). For example, in Finland, the

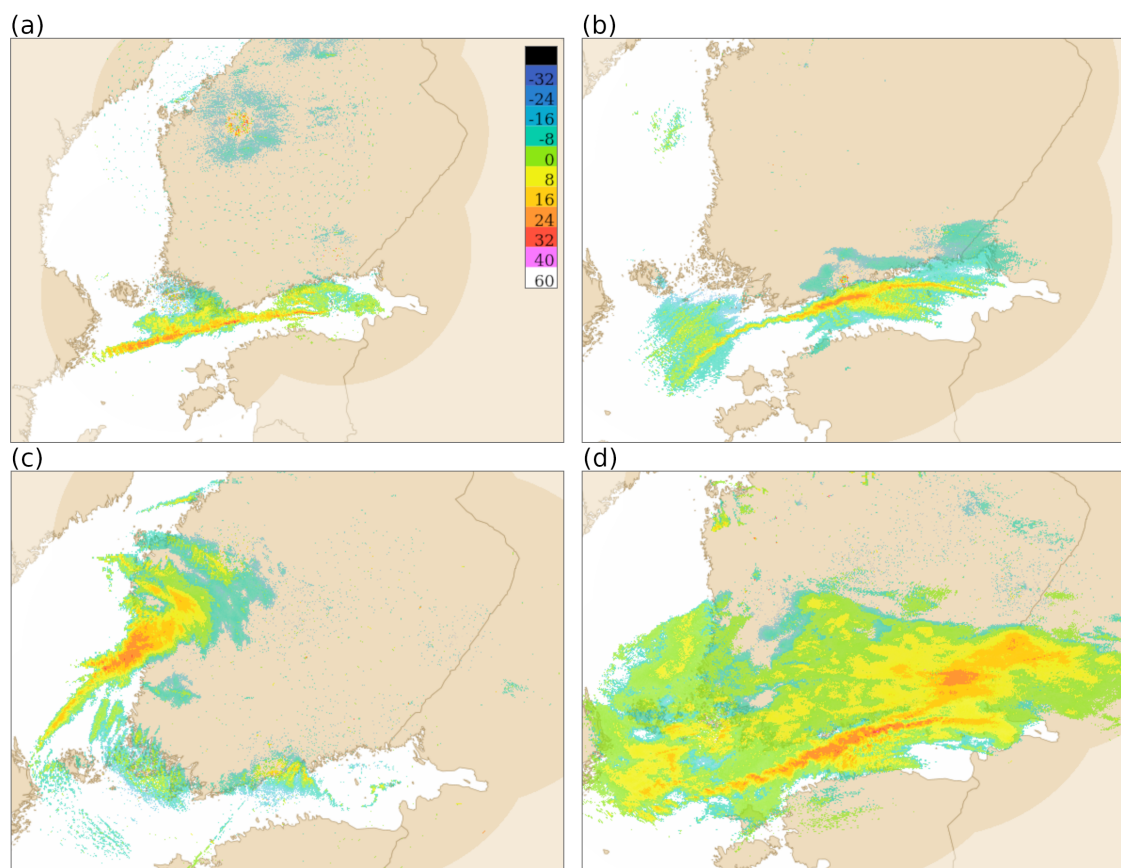


**Figure 1.** Radar reflectivity (in units of dBZ) on (a) 13 November 2007 at 15 UTC, (b) 2 February 2012 at 23 UTC, (c) 8 January 2016 at 11 UTC and (d) 8 November 2016 at 18 UTC.

current record for the highest measured daily snow depth increase (73 cm) was associated with a localized snowband making landfall over western Finland in 2016 (Olsson et al., 2017). In eastern Sweden, multiple consecutive snowbands brought 130 cm of snowfall within a few days around the town of Gävle in 1998, causing large societal impacts and economical losses (JEW2017, Westerblom, 2024). Furthermore, Japan is one of the snowiest regions globally due to frequent sea-effect snowfall (Steenburgh and Nakai, 2020). Sea-effect or lake-effect snowfall has also been observed, for example, along the Black Sea region in Turkey (Baltaci et al., 2021), the Caspian Sea (Ghafarian et al., 2018) and occasionally near the coast of the United Kingdom (Norris et al., 2013).

Existing long-term statistics on sea-effect snowbands in the Baltic Sea area have been limited to specific regions and typically constrained to prevailing wind directions that bring snowfall to the adjacent land. In Finland, OLS2022 used ERA5 reanalysis data (Hersbach et al., 2020) and snow depth observations to show that the Finnish coastline has experienced an annual average of 16 intense snowband days between 1973–2020, with most cases having occurred in November–December. Based on 11 years of data from a regional climate model, JEW2017 showed that over the eastern coast of Sweden, favorable conditions for



snowbands with northerly to easterly winds occur on approximately 4 to 7 days per year. In the study of JEW2017, the highest mean precipitation amounts during conditions favourable for sea-effect snowbands occur along the Swedish coastline of the Bothnian Bay, Bothnian Sea, and the western Gotland Basin, over Gotland, as well as over northern Poland (see regions in Fig.

2). Bednorz et al. (2022) later confirmed, through an analysis of 25 highly intense snowfall events affecting the Polish Baltic Sea coast, that typical conditions favouring the occurrence of sea-effect snowfall over the southern Baltic Sea arise when the low-level circulation brings cold, northerly air masses over the region and the low-level winds are from the northeast.

Identifying the long-term climatology of sea-effect snowfall is challenging due to the small spatial and temporal scale of the systems, often with very localized impacts, and lack of continuous observational datasets with long temporal coverage.

Snowbands are typically only a few to tens of kilometers wide, and over land the resulting snowfall may occur within only a few tens of kilometers along the coastline. Furthermore, snowbands form over the sea where observations are few. Consequently, existing climatologies for the Baltic Sea area have primarily been based on detecting snowbands by finding the environments favourable for their occurrence from gridded climate model and reanalysis datasets. Accordingly, a snowband day has been defined as a day with environmental conditions favouring sea-effect snowfall.

JEW2017 was the first to establish a set of criteria that successfully identified snowband days from gridded climate model data along the east coast of Sweden. The criteria were based on extensive literature of the atmospheric conditions known to be key factors for the occurrence of snowbands (Holroyd, 1971; Niziol, 1987; Andersson and Nilsson, 1990; Niziol et al., 1995; Laird et al., 2003). OLS2020 refined the snowband criteria to a set of conditions that statistically favour the occurrence of intense snowbands over the northern Baltic Sea. Building on the work of JEW2017, previous literature of sea-effect snowfall and the analysis of four case studies of intense snowbands over the northern Baltic Sea using a convection-permitting numerical weather prediction model, OLS2020 and OLS2022 used the following criteria. Firstly, the sea must be ice-free (with a sea surface temperature greater than 0 °C), and there should be a large vertical temperature difference (> 13 °C) between the sea surface and the 850 hPa-level. This combination of factors ensures an unstable airmass over an open water body, which is essential for generating strong surface fluxes of heat and moisture, and favors the formation of convective updrafts and sea-effect snowfall. Secondly, low-level winds should be suitable. Moderate or strong low-level wind speed is important as it will enhance surface fluxes, and is more often associated with intense convective snowbands. For the convection to organize into a long, band-like structure, low-level directional wind shear should be weak. Furthermore, the snowbands generally align parallel to the prevailing low-level winds (approximately between 1000 hPa and 700 hPa) which should be towards the coastline when focusing on bands that affect land areas. Thirdly, a deep boundary layer is necessary to support the growth of convective clouds. Lastly, to ensure that convection has initiated, snowfall must occur. If these conditions were met, a snowband day was detected from the gridded atmospheric data.

The previously made studies on snowband statistics in Finland and Sweden are based on datasets created using weather and climate models having a relatively coarse resolution, which need a parameterization scheme to represent the underlying convective processes. Recently, a 21-year climate simulation applied with 3 km horizontal grid spacing, explicitly resolving deep convection, has been generated for the Nordic region with the HARMONIE-Climate (HCLIM) regional climate model (Lind et al., 2020). Such "convection-permitting" climate models with fine resolutions have been shown to lead to signifi-

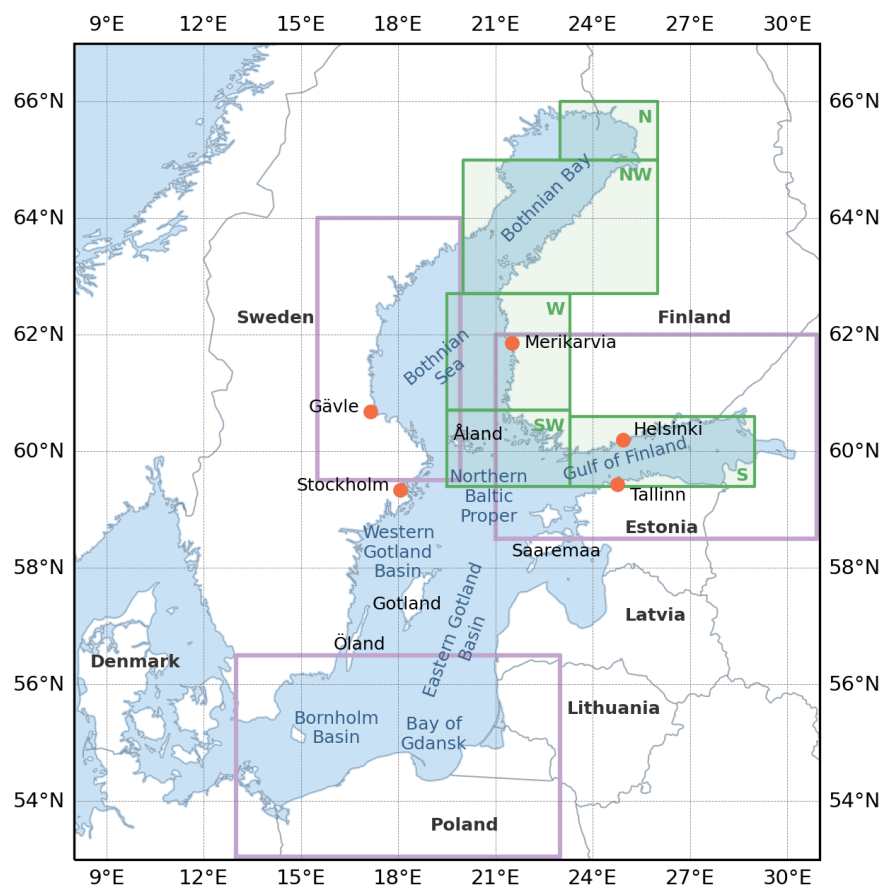


**Figure 2.** The study domain and the location of the subregions investigated in this study. Green boxes show the subregions defined by Olsson et al. (2022) and presented in Fig. 4. The shaded area corresponds to the area labeled as FI in the text. Purple boxes show the subregions presented in Fig. 10–11.

cant improvements in the representation of sub-daily convective precipitation (Lucas-Picher et al., 2021; Lind et al., 2020; Médus et al., 2022). Comparison to a wide range of observational datasets has shown that the convection-permitting HCLIM model, with reanalysis data as boundary conditions, simulates summertime daily precipitation distributions over Fennoscandia well and provides considerable added value to the statistics, amplitude and timing of hourly-scale extreme precipitation over Fennoscandia (Médus et al., 2022). The same can generally be expected for convective precipitation during the cold season.

In this study, we utilise the convection-permitting HCLIM simulation, forced by ERA-Interim reanalysis data (Dee et al., 2011), to investigate the climatology of snowband days in the Baltic Sea area in 1998–2018. The goal is two-fold. First, we examine whether HCLIM can realistically simulate snowbands. To address this, we perform a qualitative comparison with the snowband day climatology that was defined by OLS2022 using ERA5 and snow depth observations and, in addition, examine the performance of HCLIM for a set of events from the recent past. Then, we apply the kilometer-scale HCLIM dataset across



the entire Baltic Sea region to identify the general long-term spatial and temporal distribution of snowband days and the areas most at risk from sea-effect snowfall. This enables us to complement existing snowband day climatologies for Finland and Sweden and, for the first time, to develop a 21-year climatology of sea-effect snowfall environments across the full Baltic Sea area.

This study is organized as follows. The HCLIM dataset and methodology used to detect snowbands is described in Section 2. Section 3 first presents results from the comparative analysis with a previously defined climatology (Sect. 3.1) and case studies of past snowband events over the Baltic Sea (Sect. 3.2), followed by analysis of the long-term distribution of snowband days (Sect. 3.3) and associated snowfall (Sect. 3.4) over the entire Baltic Sea area. The results are discussed in Section 4 and concluding remarks provided in Section 5.

## 2 Data and methods

### 2.1 HARMONIE-Climate (HCLIM) simulation

The HCLIM regional climate model is being developed and maintained in a consortium consisting of members from several national meteorological institutes in Europe (Lindstedt et al., 2015; Belušić et al., 2020) and is the climate version of the HIRLAM-ALADIN Research on Mesoscale Operational NWP in Euromed (HARMONIE) system (Bengtsson et al., 2017). Here, we use a pre-existing 21-year km-scale simulation made with HCLIM cycle 38 over Fennoscandia for the time period of 1998-2018 (The HARMONIE Climate community, 2025). The simulation was carried out as part of the Nordic Convection Permitting Climate Projections (NorCP) project and is described in detail and evaluated in Lind et al. (2020); Olsson et al. (2021); Médus et al. (2022).

The HCLIM convection-permitting simulation has been performed in a double nested approach; in the first step the global ERA-Interim reanalysis was downscaled using the HCLIM-ALADIN configuration at 12 km spatial resolution over a domain covering a large part of Europe and the eastern North Atlantic. The HCLIM-AROME configuration was then run with 3 km spatial resolution over an area covering Fennoscandia. The lateral boundary conditions from the HCLIM-ALADIN simulation were updated every 3 hours. Both HCLIM model versions used 65 vertical levels and the SURFEX surface parameterization (Masson et al., 2013).

It should be noted that while the deep convection is treated explicitly in the convection-permitting configuration of HCLIM, the shallow convection is still parameterized. The dynamics and physics parameterizations used in HCLIM cycle 38 are described in detail in Belušić et al. (2020) and references therein.

### 2.2 Sea-effect snowfall detection method

We adopt the ingredients-based sea-effect snowfall detection method used previously by JEW2017, OLS2020 and OLS2022 to find snowband days over the Baltic Sea in September-May between 1998-2018. The detection method applies, at every 3 km  $\times$  3 km grid box and 3-hourly timestep of HCLIM output data, a set of criteria for snowfall intensity and environmental



conditions known to be favourable for the occurrence of sea-effect snowbands. If all of the criteria are fulfilled, that grid box and time step is counted as sea-effect snowfall. Days when all the criteria are fulfilled at at least one 3-hourly timestep (either in a grid box or within a subregion, see Sect. 3) are marked as snowband days. In order to accommodate the two-fold goal of this study, and to distinguish between intense snowbands and a wider range of sea-effect environments, we use three sets of criteria. The criteria are summarized in Table 1 and described in more detail below.

First, we use a similar set of criteria as OLS2022 to conduct a comparative analysis between HCLIM and the pre-existing climatology of snowband days along the Finnish coastline (Table 1, Sect. 3.1). OLS2022 divided the Finnish coastline into subregions depending on the orientation of the coast (N, NW, W, SW, S, and FI, see subregions in Fig. 2). In each grid box at every time step, criteria for sea-surface temperature, low-level temperature difference, directional wind shear, near-surface wind speed, boundary layer height, low-level wind direction and daily snowfall were checked. Low-level wind direction was required to be towards the Finnish coastline in each subregion to focus solely on cases that drift towards the Finnish land areas. The snowband criteria of OLS2022 were adopted from OLS2020, however OLS2022 additionally required that observed daily snow depth must have increased at least 2 cm somewhere over land in the subregion. We replicate the criteria of OLS2022, but without the requirement for observed snow depth. Despite this difference, for the sake of clarity, we refer to this set of criteria as "the snowband criteria of OLS2022".

Second, to investigate the climatology of snowband days over the whole Baltic Sea area with HCLIM (Sect. 3.3), we slightly refine the criteria of OLS2020 and OLS2022. Instead of daily snowfall, we use a threshold for 3-hourly snowfall (calculated from the 3-hour time period after the other criteria are fulfilled) and omit the criterion for 900 hPa-level wind direction. This ensures that the snow falls roughly at the same time as the environmental conditions are favourable for the occurrence of snowbands, increasing the likelihood that the detected cases are indeed sea-effect snowfall and not non-convective large-scale snowfall occurring earlier or later on the same day. By excluding the requirement for low-level wind direction, the study area can be expanded to the whole Baltic Sea. Even though the refined criteria do not, by default, restrict the cases to certain wind directions, the detected snowbands will be sampled according to the prevailing low-level winds in some of the regional analysis presented in Sect. 3.3 and 3.4. From hereon, we refer to this set of criteria as "the refined snowband criteria".

As in OLS2020 and OLS2022, we focus on snowbands that are associated with a notable snowfall intensity. Defining an appropriate threshold for snowfall amount to capture intense snowbands is difficult and the number of cases can be expected to be sensitive to the threshold. We select the threshold of  $0.5 \text{ mm (3h)}^{-1}$  (in liquid water equivalent) and conduct a sensitivity test to the threshold (see Sect. 3.3). This threshold is between the median and 98<sup>th</sup> percentile of 3-hourly snowfall calculated from snowy timesteps (defined as time steps with snowfall amount over  $0.01 \text{ mm (3h)}^{-1}$  when all the other refined criteria except for the snowfall criterion are fulfilled (Fig. A1). The median (98<sup>th</sup> percentile) of 3-hourly snowfall during timesteps with environmental conditions favourable for snowbands is generally between  $0.03\text{--}0.12 \text{ mm (3h)}^{-1}$  ( $0.6\text{--}1.2 \text{ mm (3h)}^{-1}$ , see Fig. A1). We note that, in this study, only snowfall is considered, whereas other solid precipitation types such as graupel are not included in the analysis.

Lastly, the above mentioned criteria adopted from previous studies have been designed to detect banded sea-effect snowfall (OLS2020, OLS2022). Sea-effect snowfall systems can take many shapes and sizes. To take into account a wider range of





**Table 1.** The criteria for meteorological parameters included in the sea-effect snowfall detection method. Note that Olsson et al. (2022, or OLS2022) included an eighth criterion for observed daily snow depth, but that criterion is not used in this study (see Section 2.2). Snowfall is given in liquid water equivalent.

	Snowband criteria of Olsson et al. (2022)	Refined snowband criteria	Loose criteria
Study area	Finland	Baltic Sea	Baltic Sea
Snowfall	$> 1.5 \text{ mm day}^{-1}$	$> 0.5 \text{ mm (3h)}^{-1}$	$> 0.5 \text{ mm (3h)}^{-1}$
Sea-surface temperature	$> 0 \text{ }^{\circ}\text{C}$	$> 0 \text{ }^{\circ}\text{C}$	$> 0 \text{ }^{\circ}\text{C}$
Difference between 850-hPa and sea-surface temperature	$> 13 \text{ }^{\circ}\text{C}$	$> 13 \text{ }^{\circ}\text{C}$	$> 13 \text{ }^{\circ}\text{C}$
Difference in wind direction between the 950-hPa and 700-hPa levels	$< 60 \text{ }^{\circ}$ , note that Olsson et al. (2022) used the 975-hPa level instead of the 950-hPa level	$< 60 \text{ }^{\circ}$	-
Near-surface wind speed	$> 7 \text{ m s}^{-1}$	$> 7 \text{ m s}^{-1}$	-
Boundary layer height	$> 1000 \text{ m}$	$> 1000 \text{ m}$	-
900-hPa level wind direction	Towards the Finnish coastline in five subregions ( $90\text{--}255^{\circ}$ in S, $135\text{--}285^{\circ}$ in SW, $200\text{--}330^{\circ}$ in W, $270\text{--}360^{\circ}$ in NW, $180\text{--}270^{\circ}$ in N, see subregions in Fig. 2.)	-	-

sea-effect snowfall environments and to test the sensitivity to the number of criteria used to detect the cases, we also include a brief analysis with a looser set of criteria. The loose criteria consider only the most important forcing mechanisms, namely, the positive sea-surface temperature and the large temperature gradient between the surface and the overlying airmass which



together drive the occurrence of strong surface fluxes of heat and moisture to the atmosphere. In addition to the sea-surface temperature and vertical temperature difference criteria, the 3-hourly snowfall rate is also included in the loose criteria analysis.

### 3 Results

#### 3.1 Comparative analysis of snowband day climatologies

155 The monthly mean numbers of snowband days, as detected from HCLIM data using the criteria of OLS2022, on one hand, and as obtained from OLS2022, on the other hand, are presented in Figure 3 for Finland (FI, see subregions in Fig. 2). Here, a snowband day is defined as a day during which the seven criteria adopted from OLS2022 are fulfilled in at least one grid box at least once per day somewhere in the subregion. Note that here only cases with wind direction favourable to bring snowfall over the Finnish coastline are included (see Table 1). The monthly distribution of snowband days in FI in HCLIM resembles  
160 that seen by OLS2022 (Fig. 3). In both data sets, snowband days are most frequent in November-January, with a peak in December. The number of snowband days is slightly higher in HCLIM than in OLS2022 in all months except for March-May, when HCLIM shows a lower number. We note that only a qualitative comparison between the current study and OLS2022 is possible as differences may arise from the different periods of investigation (1998-2018 in HCLIM and 1997-2020 or 1973-2020 in OLS2022), different spatial resolutions of the datasets (3 km in HCLIM and about 31 km in OLS2022) and lack of the  
165 criterion for observed snow depth in HCLIM. The larger number of cases in HCLIM may be, at least partly, explained by the slightly looser criteria compared to OLS2022.

The annual number of snowband days in FI varies considerably from year to year in both HCLIM and OLS2022 (Table 2). In HCLIM (1998–2018), the annual mean is 18 snowband days, with a range from 7 to 42. In OLS2022 (1973–2020), the mean is slightly lower at 16 snowband days, ranging from 6 to 40 annually.

170 Although the annual and monthly mean numbers of snowband days in FI are quite similar in HCLIM and OLS2022, differences are seen within the smaller subregions (N, NW, W, SW and S). In HCLIM, the annual mean number of snowband days is largest in S, decreased from south to north and is smallest in N (Table 2, note that the subregions vary in size and therefore quantitative comparison between the subregions is not straightforward). In OLS2022, the annual mean number of snowband days in 1973-2020 is more evenly distributed between the subregions and snowband days are most frequently detected in W  
175 (Table 2).

A closer inspection into the spatial distribution of snowband days (Fig. 4) defined using the criteria of OLS2022 shows that, in HCLIM, snowband days occur most frequently with easterly to southwesterly winds close to the southern coastline of Finland in S (with an annual average of one-to-two snowband days per 3 km × 3 km area). In that region, OLS2022 shows a similar spatial distribution of snowband days (see Fig. 1 of OLS2022). However, in OLS2022, the most active region is located  
180 off the Finnish coastline in W, where the annual mean number of snowband days with south- to northwesterly winds was up to three. In HCLIM, no clear maximum is seen in W, and the annual mean number is much smaller (0-0.5 snowband days, Fig. 4). In SW and NW, HCLIM and OLS2022 show similar spatial patterns, though OLS2022 detects more frequent snowband days. In N, HCLIM shows a local maximum near the coast, while OLS2022 records fewer events.



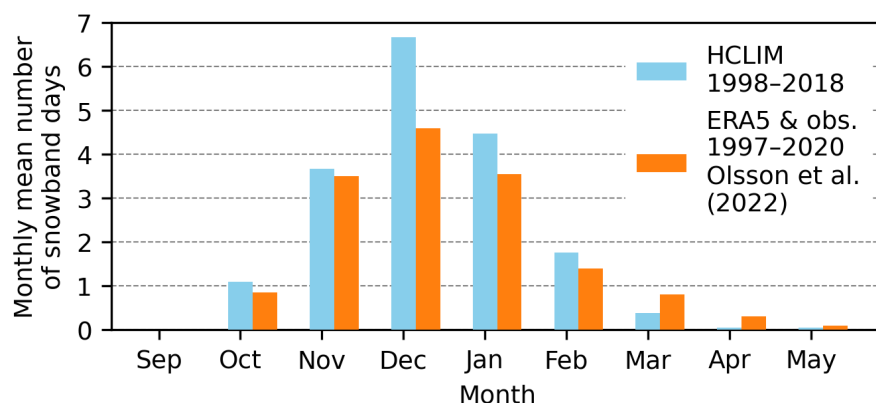


**Figure 3.** Monthly mean number of snowband days in Finland (FI, see subregion in Fig. 2) in HCLIM in 1998–2018 (blue) and that estimated from Figure 2 of Olsson et al. (2022, or OLS2022, licensed under CC BY 4.0) using ERA5 reanalysis data and snow depth observations in 1997–2020. The snowband days are detected from HCLIM using criteria close to those of OLS2022 (see Table 1). Snowband day is defined here as a day during which all the criteria were fulfilled in at least one grid box at least once a day somewhere in FI.

**Table 2.** The average, minimum and maximum annual number of snowband days in Finland. The first column shows the subregions (see Fig. 2). The second, fourth and sixth column show the number of snowband days detected in HCLIM for the period 1998–2018 using the criteria of Olsson et al. (2022, or OLS2022, criteria given in Table 1) whereas the third, fifth and seventh columns present those adapted from Table 1 of OLS2022 (licensed under CC BY 4.0) for 1973–2020. Snowband days are defined here as days when all the criteria for snowbands are fulfilled in at least one grid box at least once per day somewhere in the subregion. Snowband days that were detected in multiple subregions were included only once in FI.

	Annual average		Annual minimum		Annual maximum	
	HCLIM	Olsson et al. (2022)	HCLIM	Olsson et al. (2022)	HCLIM	Olsson et al. (2022)
FI	18	16	7	6	42	40
N	3	1	0	0	8	6
NW	4	5	0	0	11	16
W	4	7	0	1	8	18
SW	5	5	1	0	12	14
S	10	5	0	0	24	12

### 3.2 Performance of HCLIM in case studies of past snowband events

185 One observed snowband event impacting Sweden and three from Finland were selected for a closer look to explore how well HCLIM, together with two sets of snowband criteria (the refined and the loose criteria, see criteria in Table 1), perform in

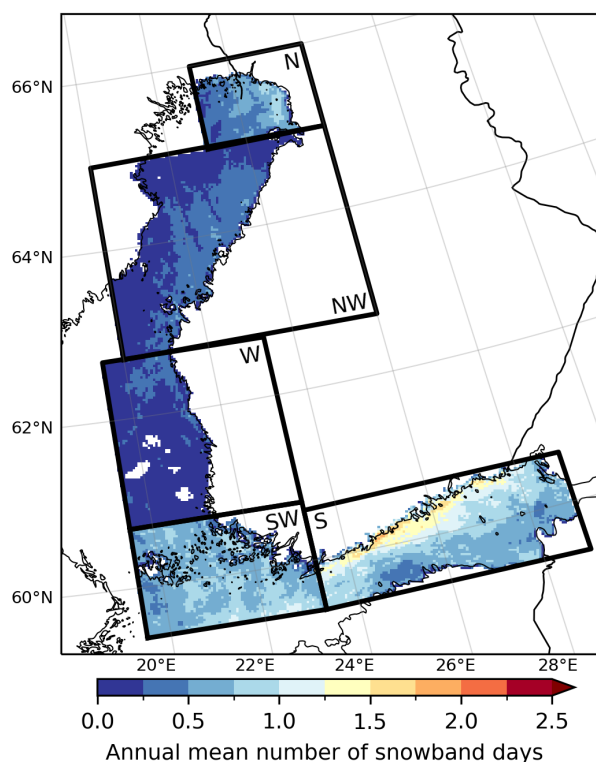


**Figure 4.** Annual mean number of snowband days in 1998–2018 in HCLIM detected by using criteria close to those used by Olsson et al. (2022, or OLS2022, criteria given in Table 1). Snowband day in each grid box is defined here as a day during which all the criteria were fulfilled at least once.

simulating and capturing banded snowfall. The events are well covered in previous literature and have been verified as sea-effect snowbands.

### 3.2.1 13 November 2007

190 The Swedish case occurred on 13 November 2007, when a long and narrow band of intense snowfall extended from the Gulf of Finland to the eastern coast of Sweden (shown at 15 UTC in Fig. 1a). We note that the snowband actually extended over land in south of Stockholm (Swedish Meteorological and Hydrological Institute, 2025), but this is not shown in Fig. 1a due to lack of radar coverage in the radar dataset used in this study. The snowband caused disruptions to traffic and slippery roads in regions south of Stockholm. In HCLIM on 13 November 2007, a snowband extended all the way from southern Finland to south of Stockholm (shown at 15 UTC in Fig. 5a), closely resembling the location and morphology of the observed system (Fig. 1a). In HCLIM, the narrow snowband prevailed throughout the day and the majority of the system was detected by both the refined and loose criteria (Fig. 5b-c).

195

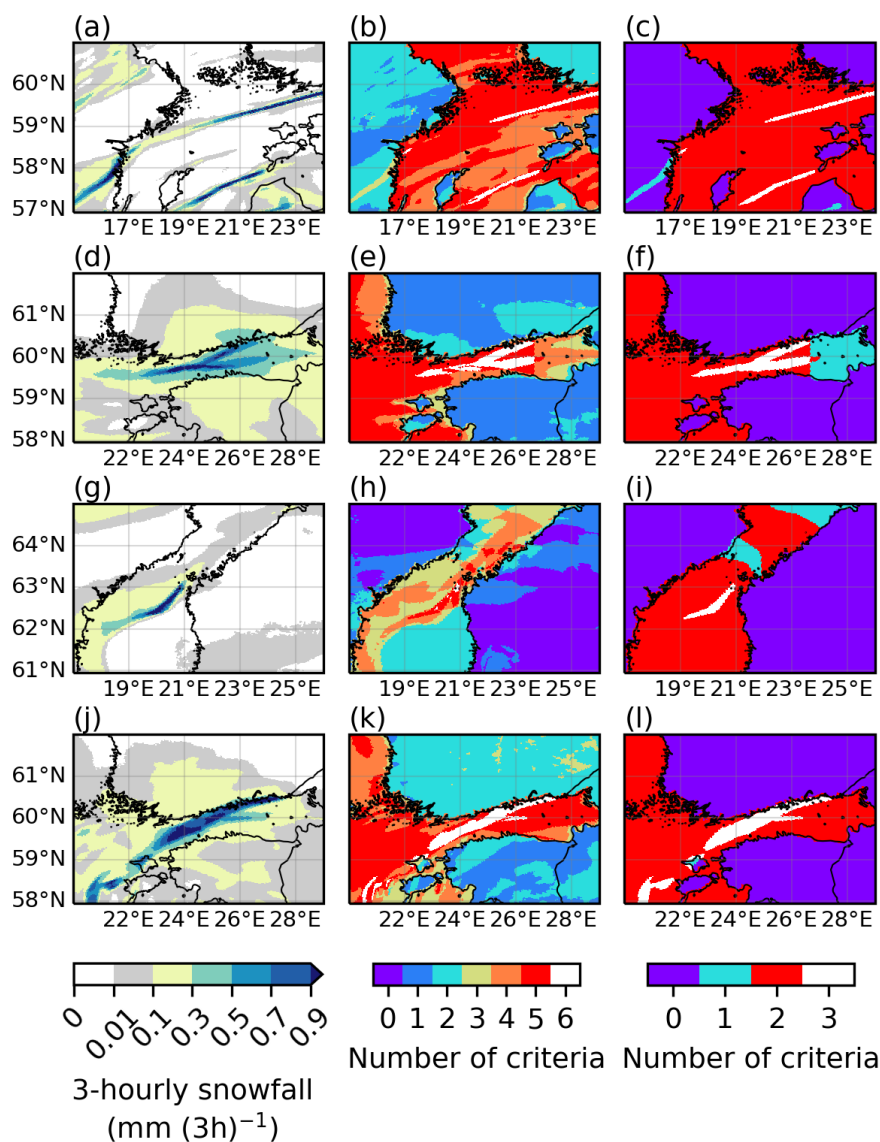


**Figure 5.** 3-hourly snowfall (mm (3h)<sup>-1</sup>, left panel), the number of refined (middle) and loose (right) criteria fulfilled at each grid box in HCLIM on (a)–(c) 13 November 2007 at 15 UTC, (d)–(f) 2 February 2012 at 15 UTC, (g)–(i) 9 January 2016 at 0 UTC and (j)–(l) 8 November 2016 at 15 UTC.

### 3.2.2 1–4 February 2012

On 1–4 February 2012, multiple snowbands formed over the Gulf of Finland (shown at 23 UTC on 2 February 2012 in Fig. 200 1b). On 3 February, a snowband drifted over the well-populated southern Finland (not shown), causing a moderate snow



accumulation around 10 cm but several hundred traffic accidents and multiple injured persons (Juga et al., 2014; Niemelä, 2012; Mazon et al., 2015, OLS2020). Between 1–4 February 2012, HCLIM simulated multiple snowbands over the Gulf of Finland (shown only on 2 February at 15 UTC in Fig. 5d). On 2 February, the location and morphology of the simulated snowband closely resembles that from the radar image (Fig. 1b), even representing the double-banded structure of the observed system (Fig. 5d). The refined and loose criteria were able to capture most of the snowband (Fig. 5e–f). On 3 February 2012, HCLIM simulated a band of snowfall impacting the southern coast of Finland but the resulting snowfall was so weak that only a few grid points fulfill the refined snowband criteria (not shown). This is partly due to the relatively high threshold for 3-hourly snowfall amount (see Sect. 2.2).

### 3.2.3 8 January 2016

On 8 January 2016, a highly local snowband hit the area of Merikarvia in the western coast of Finland. The snowband resulted in the highest recorded daily snow depth increase (73 cm), but little damage (shown at 11 UTC in Fig. 1c, Olsson et al., 2017, OLS2020). HCLIM simulates a narrow snowband travelling northeasterly across the Bothnian Sea towards the Finnish coastline on 8 January 2016 (not shown), as was the case in the actual Merikarvia case (Olsson et al., 2017). However, in HCLIM, the snowband did not make landfall until a day later on 9 January (shown at 0 UTC in Fig. 5g). The landfall occurred in the same general area of western Finland, but the simulated impact region was slightly to the north of the observed system. Although both the refined and loose criteria captured the snowband, only a few grid boxes fulfilled the refined criteria (Fig. 5h–i).

### 3.2.4 2–9 November 2016

On 2–9 November 2016, multiple intense snowbands formed over the Gulf of Finland, with a pronounced snowband drifting over the southern coast of Finland at the end of the episode (shown at 18 UTC on 8 November in Fig. 1d). In HCLIM, multiple consecutive banded snow systems formed over the Gulf of Finland in the beginning of November 2016. On 8 November 2016, HCLIM shows a snowband closely resembling that from the radar image (shown at 15 UTC in Fig. 5j). The refined and loose criteria were able to capture part of the systems on 2–3 and 5–9 November 2016 (shown on 8 November in Fig. 5k–l).

### 3.2.5 Summary

Comparison of weather radar images (Fig. 1) and snowfall simulated by HCLIM shows that the four cases are well represented by HCLIM (Fig. 5). While HCLIM captures the general characteristics of the observed sea-effect systems well, differences with respect to the radar images do occur in their exact location, timing, spatial extent and morphology. This is expected, as climate model simulations, even though using reanalysis data for lateral boundary conditions, are not designed to reproduce accurately the exact timing and location of observed events (Olsson et al., 2021). Instead, they are intended to represent long-term statistical patterns with reasonable accuracy. The refined criteria are able to capture snowband days in the correct general impact areas on 13 November 2007, 1–4 February 2012, 8–9 January 2016 and 2–3 and 5–9 November 2016. The



refined criteria do not always capture the entire areal extent or the duration of the individual snowbands. This is expected and partly due to the relatively high threshold for 3-hourly snowfall amount. Even though using a high threshold may lead to weaker convective systems being missed altogether, it is needed to detect the snowbands embedded within weaker, large-scale snowfall (see e.g. Fig. 5d–e and j–k). The systems detected by the looser criteria closely resemble the refined snowband criteria, but the areal and temporal extent of the grid boxes detected by the loose criteria is higher.

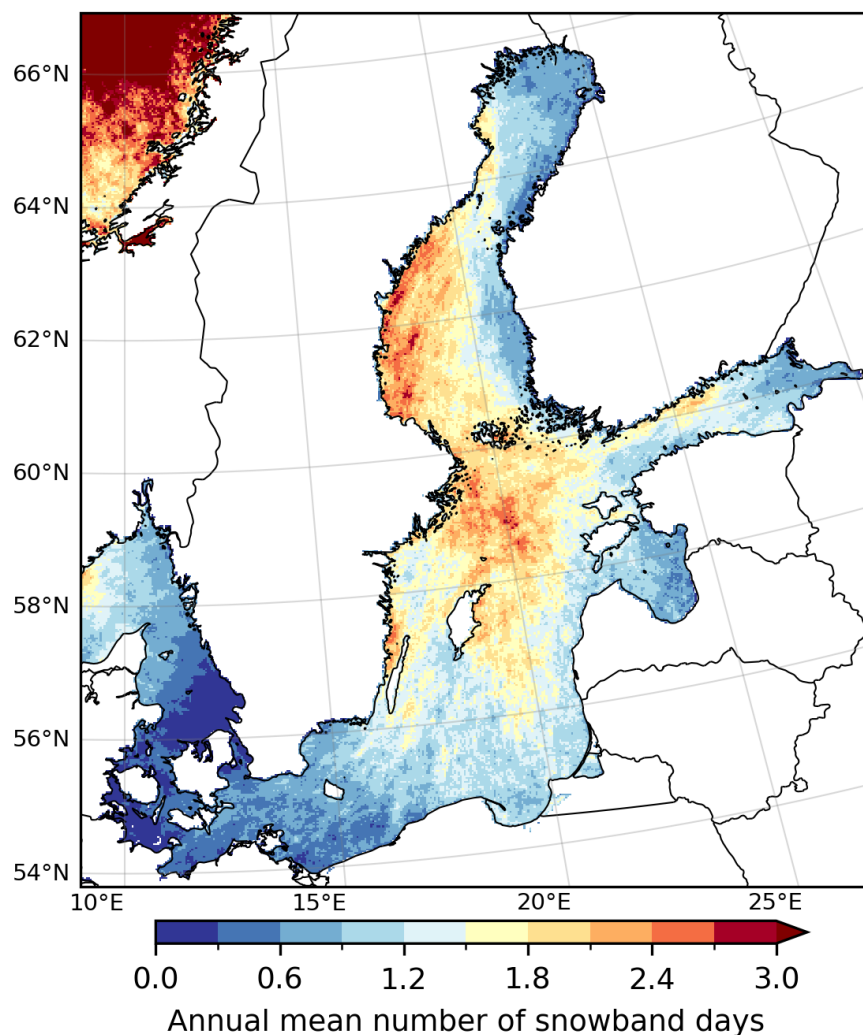
### 3.3 Frequency of sea-effect snowfall over the Baltic Sea

Figure 6 shows the annual mean number of snowband days in each grid box over the Baltic Sea area, detected from HCLIM data with the refined snowband criteria (see Table 1). According to HCLIM, snowband days over the Baltic Sea area occur most frequently near the eastern coast of Sweden, over the Northern Baltic Proper and over the Gulf of Finland (Fig. 6; for the locations, see Fig. 2). Fewer but still considerable numbers of snowband days are detected also over the southern Baltic Sea close to the northern coast of Poland.

The prevailing wind direction determines, to a large degree, whether snowbands can drift from sea to land. The snowband days in each grid box in Figure 6 were classified into four wind sectors based on the 900 hPa-level wind direction. Figure 7 indicate that snowband days over the Baltic Sea are most common when the wind has an easterly component (Fig. 7a–b) and the highest number of snowband days is typically found near the shores that are perpendicular to winds from 0–180° (Fig. 7a). Northerly-to-southeasterly winds over open sea favor the occurrence of sea-effect snowfall because they typically transport cold arctic or continental airmasses from the east to the Baltic Sea area and increase the vertical temperature difference between the surface and the overlying airmass. When the low-level wind has a westerly component (winds are from 180–360°) the number of snowband days in all regions, except for the southern and southeastern Baltic Sea, is smaller, and snowband days are most favoured in the Northern Baltic Proper, Eastern Gotland Basin and Bay of Gdansk (Fig. 7c–d). The annual number of snowband days detected in seven subregions of the Baltic Sea (see subregions in Fig. 7a) in 1998–2018 is collected into Table 3. Note that in Table 3, the size of each subregion varies and therefore the numbers between regions are not directly comparable.

**Table 3.** The average, and minimum and maximum (in brackets), annual number of snowband days in HCLIM in 1998–2018 in the subregions shown in Figure 7. The snowband days are detected using the refined snowband criteria but with an additional criterion for the 900 hPa-level wind direction between 0–90°, 90–180°, 180–270° or 270–360°. Snowband day is defined here as a day during which all the criteria are fulfilled in at least one grid box at least once per day somewhere in the subregion.

	I	II	III	IV	V	VI	VII
0–90°	7 (0, 13)	13 (0, 27)	17 (2, 33)	8 (0, 23)	14 (1, 34)	9 (0, 19)	14 (1, 32)
90–180°	4 (0, 11)	6 (0, 20)	8 (0, 23)	7 (1, 22)	4 (0, 17)	5 (0, 20)	5 (0, 20)
180–270°	3 (0, 10)	4 (0, 12)	4 (0, 11)	5 (1, 11)	2 (0, 11)	6 (0, 16)	7 (1, 23)
270–360°	2 (0, 5)	4 (0, 13)	10 (1, 25)	5 (1, 12)	8 (2, 18)	10 (0, 24)	13 (1, 25)



**Figure 6.** Annual mean number of snowband days in 1998–2018 in HCLIM detected by using the refined snowband criteria (see criteria in Table 1). Snowband day in each grid box is defined here as a day during which all the criteria were fulfilled at least once.

Snowband days over the Baltic Sea area occur mainly between October–March (Fig. 8b–g), however, the seasonal cycle varies between different regions. Over the northernmost Baltic Sea, snowband days occur primarily between October–December (Fig. 8b–d). Southward, over the Bothnian Sea, Gulf of Finland and Northern Baltic Proper, the average season is between November–February (Fig. 8c–f). The southern parts of the Baltic Sea typically experience snowband days slightly later, between December–March (Fig. 8d–g). The seasonal cycle of snowband days is governed, to a large part, by the seasonal cycle in air and sea-surface temperatures as sea-effect snowfall cannot occur if the sea is covered in ice or the airmass is too warm. However, there is considerable inter-annual variability in the sea-ice extent (see Vihma and Haapala, 2009, and references therein) and



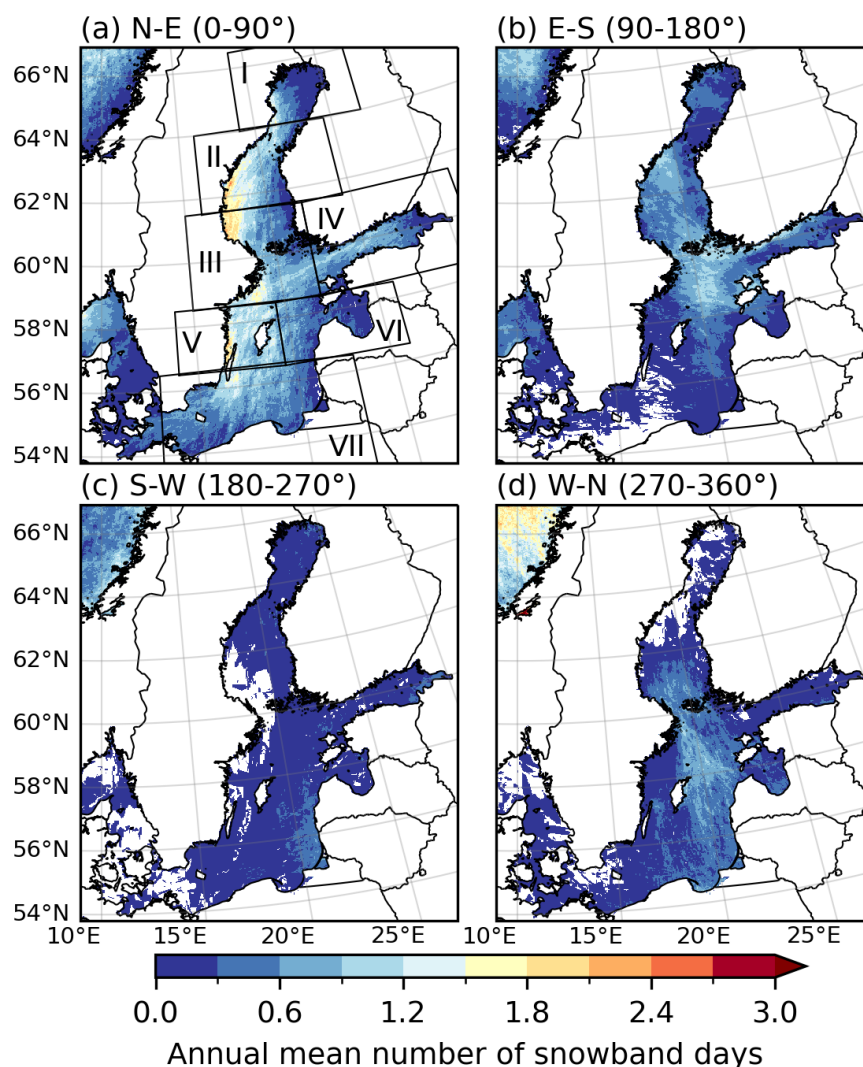


**Figure 7.** As in Figure 6, but with an additional criterion for the 900 hPa-level wind direction between (a) 0–90°, (b) 90–180°, (c) 180–270° and (d) 270–360°. The subregions presented in Table 3 and Figure 9 are marked in (a).

the number of snowband days (Table 2-3). During warmer winters, the sea ice may cover only part of the Gulf of Bothnia and Gulf of Finland whereas in severe winters sea ice may extend to large parts of the Eastern Gotland Basin (Vihma and Haapala, 2009).

The number of detected days is somewhat sensitive to the number of criteria and the thresholds used in the detection method (OLS2020, OLS2022). When the looser set of criteria (see Table 1) is used, the number of detected days is higher (Fig. A2) compared to the refined criteria (Fig. 6), however, the spatial distribution in both cases is similar. This confirms that the

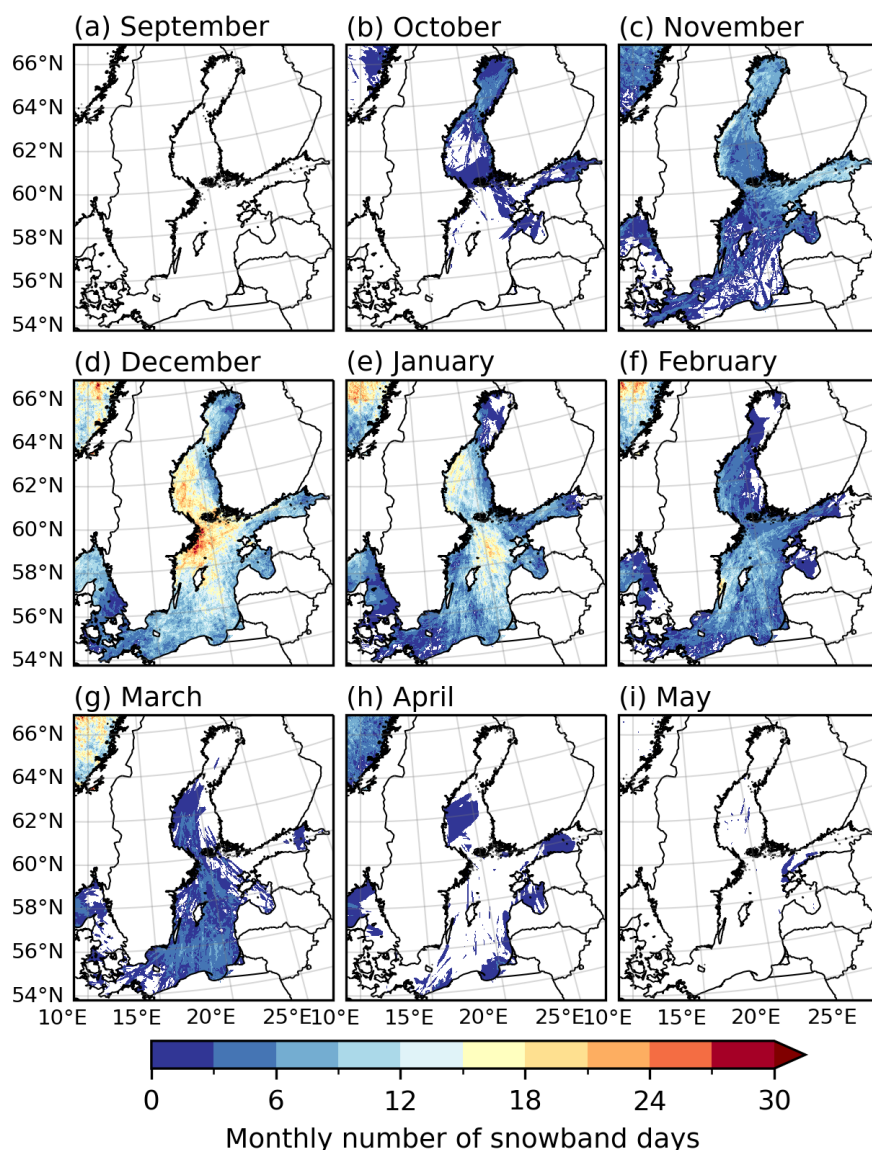


**Figure 8.** As in Figure 6, but for the total monthly number of snowband days.

general distribution of snowband days is primarily determined by the distribution of sea-surface temperature and the vertical temperature difference between the sea-surface and the lower troposphere. Lastly, the snowfall threshold used in this study was set to be quite high. When the 3-hourly snowfall threshold in the refined snowband criteria is lower (higher), the number of detected cases is higher (lower), but the spatial distribution is generally similar (Fig. A3).



### 3.4 Snowfall on snowband days

The most impactful snowbands are those that move over land. In order to estimate the snowfall distribution associated with snowband days over land and to identify the areas that receive most snowfall, we divide the Baltic Sea area into seven subregions and study the mean daily snowfall calculated from snowband days occurring in each region (Fig. 9). The snowband days are divided into four wind sectors as in Figure 7 since the prevailing wind direction determines the movement direction of snowbands and the potential impact region over the coastline. Figure 9 shows that the mean daily snowfall on snowband days is generally higher over land than over the sea. In downwind facing coastlines over land, snowfall is generally most intense near the coastline. The highest mean amounts (up to  $2.7 \text{ mm day}^{-1}$  in liquid water equivalent) occur over the eastern coast of Sweden with winds from  $90\text{--}180^\circ$  (Fig. 9b).

Note that not all snowbands in Fig. 9 drift over land and that some of the detected days likely include also non-convective snowfall occurring on snowband days. In Fig. 9, attention should be focused mainly on the coastlines that are downwind of the prevailing wind direction. Considerable snow amounts are seen for example over the eastern coast of Sweden over land in region V with winds from  $180\text{--}270^\circ$ , which include wind directions pointed away from the coastline and that generally do not favor snowbands in those regions (Fig. 7c, Table 3). The snowfall may have been sampled due to an approaching low-level system with large-scale snowfall occurring before or after a snowband was detected in the subregion. On the other hand, convective snowbands may also be embedded within low-pressure related large-scale snowfall (see e.g. Saarikivi, 1989). Thus, the daily total snow amount on snowband days can often be a combination of both localized intense convective snowfall and weaker large-scale snowfall.

Three regions with numerous snowband days in Fig. 7 and high mean snowfall (Fig. 9) are chosen for a more detailed investigation. Figures 10 and 11 show the 98<sup>th</sup> percentile of daily snowfall and the number of days with daily snowfall exceeding  $5 \text{ mm day}^{-1}$  on snowband days over northeastern coast of Sweden (Fig. 10a, 11a), southern coast of Finland (Fig. 10b, 11b) and northern coast of Poland (Fig. 10c, 11c). Note that in Fig. 10-11, low-level winds have been restricted to be towards the coastline. Figure 10 shows that Finland and Poland generally experience more moderate (98<sup>th</sup> percentile is up to  $5\text{--}6 \text{ mm day}^{-1}$  in liquid water equivalent) snowfall than Sweden (over  $8 \text{ mm day}^{-1}$ ). The same holds true also for the number of days with snowfall exceeding  $5 \text{ mm day}^{-1}$ , namely, some regions in the Swedish coastline experience up to 25 days whereas Finland and Poland experience only up to ten during the 21-year long time period.

## 4 Discussion

In this study, snowband days over the Baltic Sea area occur most frequently near the east coast of Sweden, over the Gulf of Finland and Northern Baltic Proper (Fig. 6). Snowband days are most prevalent when the low-level winds have an easterly component (i.e. 900 hPa-level wind direction is between  $0\text{--}180^\circ$ , Fig. 7a–b, Table 3). The HCLIM-based snowband climatology resembles the 11-year climatology of snowbands for Sweden, being simulated with another, coarser-resolution, regional climate model by JEW2017. They showed that when the low-level wind was from  $0\text{--}90^\circ$ , hotspots for precipitation on days with favourable conditions for convective snowbands typically occurred over land in the Swedish coast of the Bothnian Sea and

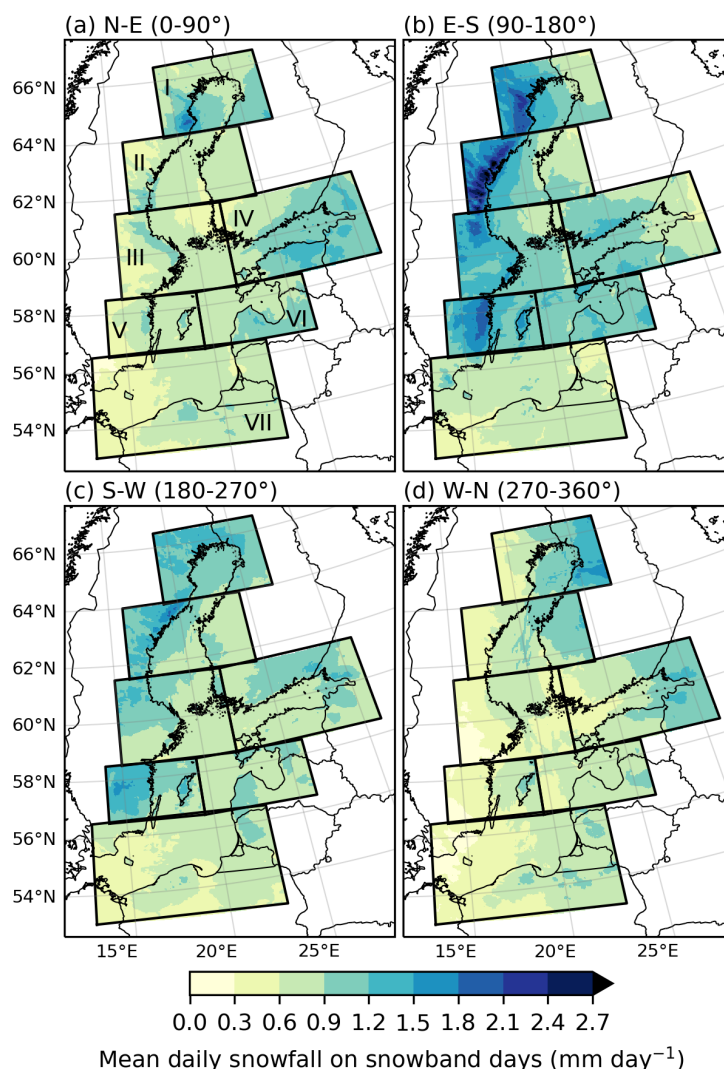


**Figure 9.** Mean daily snowfall on snowband days in seven subregions of the Baltic Sea area. The snowband days are detected using the refined snowband criteria but with an additional criterion for the 900 hPa-level wind direction between (a) 0–90°, (b) 90–180°, (c) 180–270° or (d) 270–360°. Snowband day in each subregion is defined here as a day during which all the criteria were fulfilled in at least one grid box at least once per day somewhere in the subregion.

Western Gotland Basin, as well as in Gotland (see Fig. 4 in JEW2017). In majority of those regions, mean daily snowfall was between 2  $\text{mm day}^{-1}$  (JEW2017). Local maxima in mean daily snowfall on snowband days (mean daily snowfall between roughly 0.9-2.1  $\text{mm day}^{-1}$ ) are also seen in the abovementioned regions in the current study (Fig. 9a–b). Furthermore, although less frequent, snowbands in HCLIM are also detected over the southern Baltic Sea, where they are mostly associated with northwesterly to northeasterly winds and typically occur between November-March (Fig. 8). This is consistent with the findings

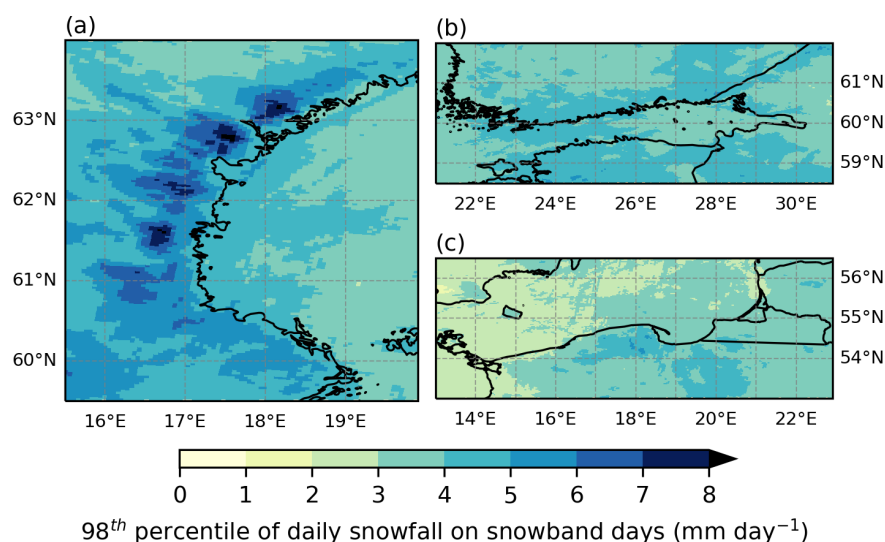


**Figure 10.** 98<sup>th</sup> percentile of daily snowfall on snowband days in the three subregions shown in Fig. 2. Snowband day in each subregion is defined here as a day during which all the refined snowband criteria (see Table 1) were fulfilled, and the 900 hPa-level wind direction was (a) 350–360° or 0–140°, (b) 90–255° and (c) 280–360° or 0–80°, in at least one grid box at least once somewhere in the subregion.

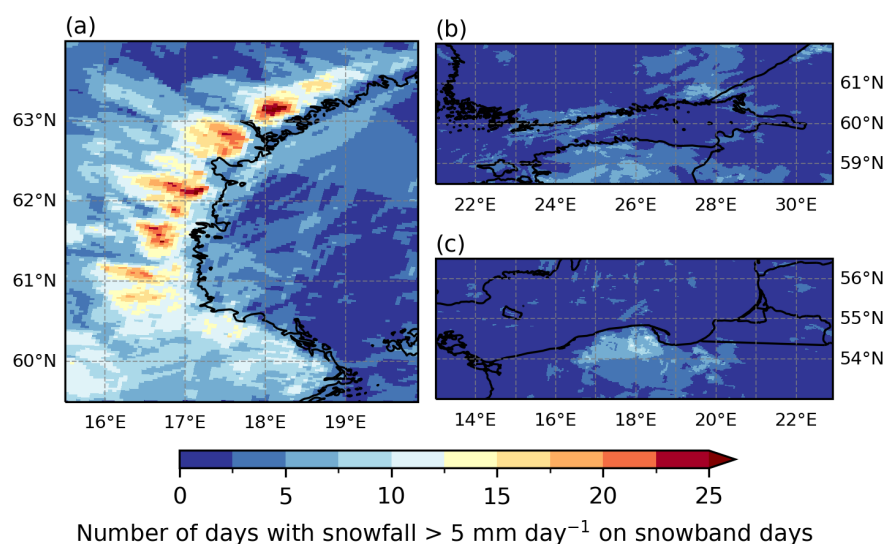


**Figure 11.** As in Figure 10, but for the number of days with snowfall exceeding 5 mm day<sup>-1</sup> on snowband days.

of Bednorz et al. (2022), who documented typical conditions linked to 25 extreme snowfall events occurring over northern Poland. The extreme cases (that led to observed snow depth increase of at least 20 cm within two days) occurred between





November-February, typically under a northeasterly circulation in the lower troposphere over warm sea water. In the current study, a local maximum in daily snowfall (98<sup>th</sup> percentile between 4–5 mm day<sup>-1</sup> in liquid water equivalent) on snowband days with winds towards the Polish coastline was found near the northern coast of Poland (Fig. 10).

315 The snowband day climatology near the Finnish coastline also shares several similarities with the previously defined climatology of OLS2020 and OLS2022. When the criteria of OLS2022 were applied to HCLIM data, the annual mean number and monthly distribution of snowband days in Finland closely resembled those shown by OLS2022 (Table 2, Fig. 3). Snowband days in HCLIM occurred most frequently along the southern coast of Finland in S, consistent with the main hotspots reported in OLS2022.

320 A notable difference between the current study, OLS2020 and OLS2022, however, was seen in the location of the most favourable region for snowband occurrence. While OLS2020 and OLS2022 found that the most favourable region for snowband occurrence was near the western coast of Finland (region W) during southerly-to-westerly winds, this maximum in occurrence frequency is absent in HCLIM (Fig. 4, Fig. 7). In fact, westerly winds were found to be the least favourable for snowband occurrence across the northern Baltic Sea in HCLIM (Fig. 7c–d).

325 The reason for this discrepancy is not fully understood. On one hand, HCLIM has a superior spatial resolution (3 km) and explicitly resolves deep convection, which allows it to represent convective updrafts more accurately than the datasets used by OLS2020 and OLS2022. Namely, OLS2020 used regional climate model data with 11 km resolution and parameterized deep convection, whereas OLS2022 used the ERA5 reanalysis data at 31 km resolution, which exceeds the size of the smallest sea-effect snowfall systems. This leads to uncertainty in the representativeness of snowbands in those datasets. For example, over the Great Lakes area, Notaro et al. (2015); Lucas-Picher et al. (2017) have shown that climate models with grid spacings  
330 larger than 10 km were not able to accurately represent all lake-effect snowfall events. On the other hand, OLS2022 showed that ERA5 was able to successfully capture past well known cases of sea-effect snowfall.

Four case studies from the northern Baltic Sea revealed that HCLIM was able to simulate past high-impact snowbands well and the sea-effect snowfall detection method captured the events. The case studies and comparison to the previous climatology by OLS2022 support the use of HCLIM and the refined snowband criteria to identify the general occurrence distribution  
335 of snowband days and areas most at risk from convective snowfall over the Baltic Sea area. However, it should be kept in mind that the detection method does not explicitly find convective precipitation and, instead, is based on finding days with considerable snowfall and environmental conditions that favor the occurrence of snowbands. It is therefore possible that some of the detected snowband days that form the snowband day climatology did not actually involve convective precipitation forced by the sea-effect. On the other hand, some cases may be undetected if the criteria used by the detection method are too strict.

## 340 5 Conclusions

In this study, we use the convection-permitting HCLIM climate model data at 3 km horizontal and 3-hour temporal resolution to study the long-term occurrence of snowband days over the Baltic Sea area in 1998–2018. To accomplish this goal, we utilize a refined sea-effect snowfall detection method that finds the grid boxes and time steps with considerable snowfall (3-hourly





snowfall over 0.5 mm) and environmental conditions known to be favourable for the occurrence of snowbands (see criteria in Table 1).

According to HCLIM, snowband days (i.e. days when all the refined snowband criteria are fulfilled at least once) are most frequent near the east coast of Sweden, southern coast of Finland and between Sweden and Estonia (up to a few snowband days per year in a 3 km × 3 km area) and when the low-level wind has an easterly component. Over the northern Baltic Sea, the snowband season typically begins in October and ends in February. Over the southern Baltic Sea, snowband days are favoured by low-level winds having a northerly component and occur typically between December–March. A more detailed summary of the key findings for different regions of the Baltic Sea is as follows:

- Gulf of Bothnia between Sweden and Finland: Snowband days typically occur in October–January over the Bothnian Bay in the north and in November–February over the Bothnian Sea in the south, most frequently near the eastern coast of Sweden, and with low-level winds from 0–180°. On snowband days, mean daily snowfall is highest near the Swedish coastline. Daily snowfall over 8 mm day<sup>-1</sup> (98<sup>th</sup> percentile, liquid water equivalent) is seen near Sweden over the Bothnian Sea when low-level winds are towards the coastline.
- Gulf of Finland between Finland and Estonia: Most snowband days occur between November–February and with low-level winds from 0–180°. Considerably fewer snowband days are seen with westerly winds. On snowband days with low-level winds towards the Finnish coastline, daily snowfall is over 6 mm day<sup>-1</sup> (98<sup>th</sup> percentile, liquid water equivalent) near the coastline.
- Northern Baltic Proper between Sweden, Finland and Estonia: Snowband days are detected mainly between November–March, peaking between December–January and occur mainly with low-level winds from 0–180° and 270–360°.
- Southern Baltic Sea: Snowband days are most common near the east coast of Sweden and near the coast of Poland and Lithuania. The average season spans December–March. Low-level winds from 0–90° favor snowband days near Sweden. Over the southernmost Baltic Sea near the Bay of Gdansk, snowband days occur mostly with winds from 0–90° and 270–360°.

Four case studies of verified past sea-effect snowfall systems in the Baltic Sea area show that HCLIM, with reanalysis data used for lateral boundary conditions, is able to simulate the location and morphology of the snowbands surprisingly well. The detection method, with the refined snowband criteria, was able to capture snowband days in the correct general impact areas. Furthermore, the long-term occurrence distribution presented in this study is generally in line with past regional climatologies presented in other studies. This supports the use of the kilometer-scale regional climate model HCLIM, that has previously been shown to lead to considerable added value in the representation of summertime extreme precipitation, also in studies of past and future distributions of convective snowfall in northern Europe.

We note that the methodology used to construct the snowband day climatology has some limitations. The detection method does not explicitly seek for convective precipitation. Instead, the environmental conditions need to fit the criteria defined in previous studies of sea-effect snowfall for the snow system to be included in the snowband day climatology. The criteria consist



of quantitative thresholds for different meteorological parameters, which the number of detected days is sensitive to. Therefore, the method might miss some snowbands if the criteria are too strict, or capture non-convective snowfall if the criteria are too loose. Furthermore, although HCLIM represents previously defined snowband climatologies well, the model may contain  
380 uncertainties and biases that affect the long-term statistics. The 21-year period of investigation is rather short for studying long-term statistics, especially that of extremes, and the occurrence distribution may include uncertainty due to natural spatial and temporal variability of the snowbands.

The number of detected snowband days was shown to be sensitive to the number of criteria, however, the general characteristics of the occurrence distribution remained largely unchanged. This suggests that the spatial distribution of snowband  
385 days is primarily determined by the distribution of sea-surface temperature and the vertical temperature difference between the sea-surface and the lower troposphere. Understanding how climate change affects the extent and annual cycle of sea ice—as well as the co-occurrence of ice-free sea and cold lower-tropospheric air masses—can thus provide valuable insights into how the general characteristics and spatial distribution of sea-effect snowfall may change in the future.

This study presents, for the first time, the climatology of snowbands environments over the full Baltic Sea region. Such a  
390 climatology is important as it can be used to identify areas most at risk from sea-effect snowfall and can thus support in the planning and implementation of climate adaptation measures and be used, for example, to support operational forecasting of snowbands. The results form the fundamental basis for studying impacts of future climate change on the occurrence, frequency and intensity of sea-effect snowfall in northern Europe.

<https://doi.org/10.5194/egusphere-2025-3663>

Preprint. Discussion started: 14 August 2025

© Author(s) 2025. CC BY 4.0 License.



## Appendix A

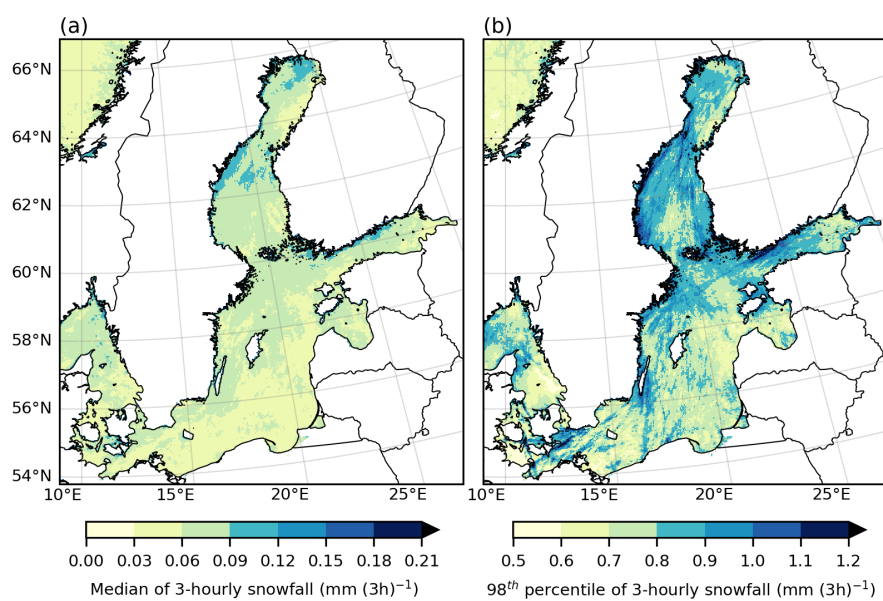


**Figure A1.** (a) Median and (b) 98<sup>th</sup> percentile of 3-hourly snowfall in 1998–2018 in HCLIM. The median and the 98<sup>th</sup> percentile of snowfall is calculated from time steps when all the refined criteria shown in Table 1 (except the criterion for 3-hourly snowfall exceeding 0.5 mm) are fulfilled and at least some snowfall occurs (i.e. 3-hourly snowfall rate exceeds 0.01 mm (3h)<sup>-1</sup>).

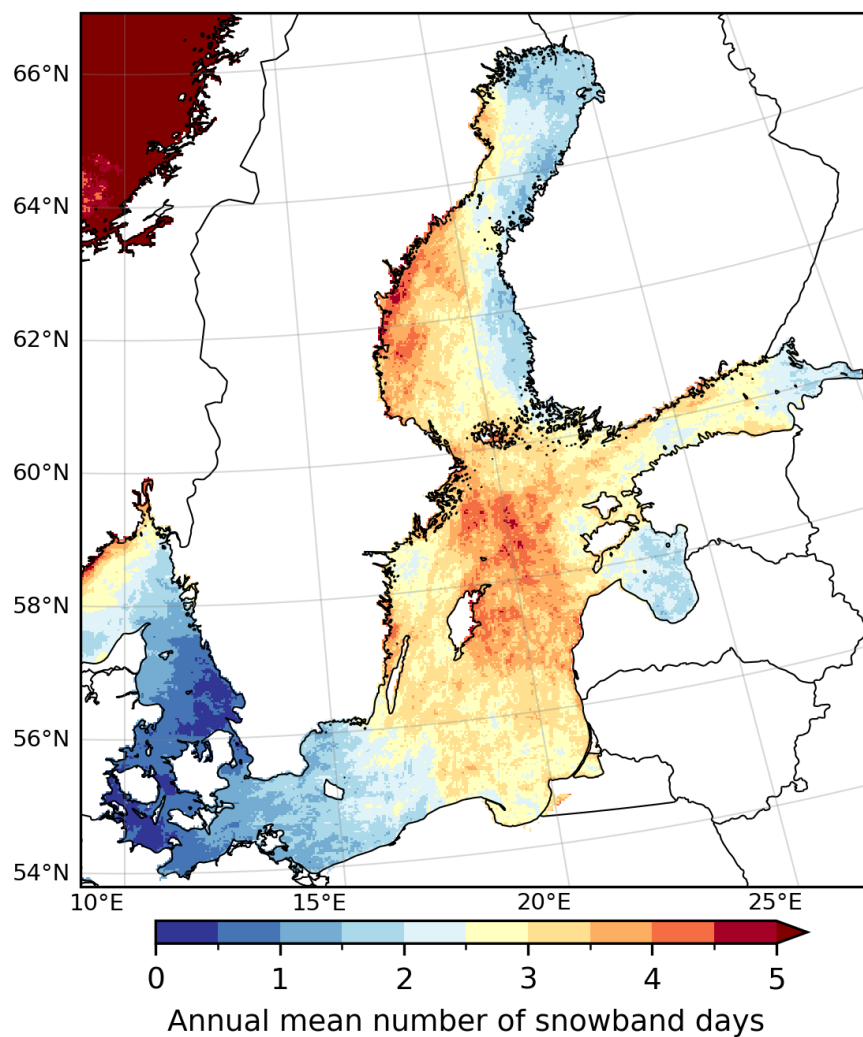


**Figure A2.** Annual mean number of snowband days in 1998–2018 in HCLIM detected by using the loose criteria (see criteria in Table 1). Snowband day in each grid box is defined here as a day during which all the criteria were fulfilled at least once.

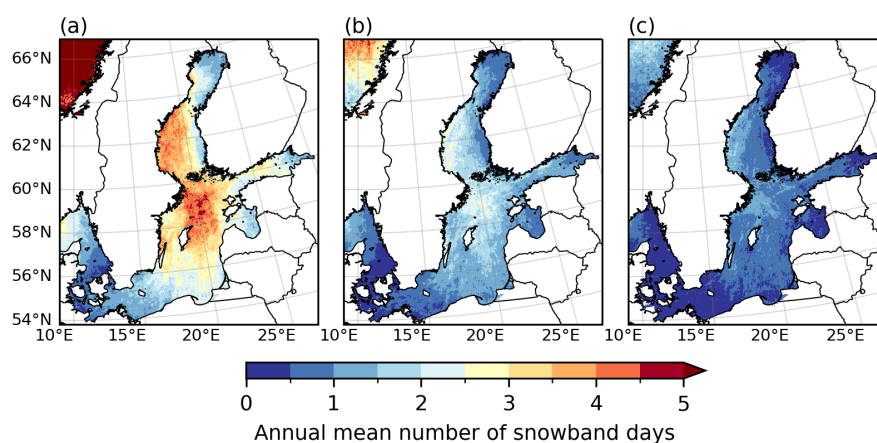


**Figure A3.** Annual mean number of snowband days in 1998–2018 in HCLIM detected by using the refined snowband criteria, but with the threshold for 3-hourly snowfall being (a)  $0.3 \text{ mm (3h)}^{-1}$ , (b)  $0.5 \text{ mm (3h)}^{-1}$  and (c)  $0.8 \text{ mm (3h)}^{-1}$ . Snowband day in each grid box is defined here as a day during which all the criteria were fulfilled at least once.





395 *Data availability.* Data is available upon request from the authors.

*Author contributions.* MV, TO and KJ conceptualized the study and analysed the data; PL produced and validated the original model data; MV and PL visualized the results; MV wrote the original draft; TO, KJ and PL reviewed and edited the manuscript.

*Competing interests.* The authors declare that there are no competing interests.

400 *Acknowledgements.* We thank Dr. Antti Mäkelä for the valuable feedback and comments on an earlier version of the manuscript. This work uses data from the NorCP project, which is a Nordic collaboration involving climate modeling groups from the Danish Meteorological Institute (DMI), Finnish Meteorological Institute (FMI), Norwegian Meteorological Institute (MET Norway) and the Swedish Meteorological and Hydrological Institute (SMHI). We thank the CSC - IT Center for Science for the computational resources to conduct the analysis. ChatGPT was used for editing the grammar and fluency in some parts of this manuscript. This research was funded by the Finnish State Nuclear Waste Management Fund (VYR) through the MAWECLI project (Dnro SAFER 6/2023, 8/2024 and 5/2025) in the SAFER2028  
405 programme.



## References

- Andersson, T. and Nilsson, S.: Topographically induced convective snowbands over the Baltic Sea and their precipitation distribution, *Weather and Forecasting*, 5, 299–312, 1990.
- Baltaci, H., da Silva, M. C. L., and Gomes, H. B.: Climatological conditions of the Black Sea-effect snowfall events in Istanbul, Turkey, *International Journal of Climatology*, 41, 2017–2028, <https://doi.org/10.1002/joc.6944>, 2021.
- 410 Bednorz, E., Czernecki, B., and Tomczyk, A. M.: Climatology and extreme cases of sea-effect snowfall on the southern Baltic Sea coast, *International Journal of Climatology*, pp. 1–15, <https://doi.org/10.1002/joc.7546>, 2022.
- Belušić, D., de Vries, H., Dobler, A., et al.: HCLIM38: a flexible regional climate model applicable for different climate zones from coarse to convection-permitting scales, *Geoscientific Model Development*, 13, 1311–1333, <https://doi.org/10.5194/gmd-13-1311-2020>, 2020.
- 415 Bengtsson, L., Andrae, U., Aspelien, T., et al.: The HARMONIE–AROME Model Configuration in the ALADIN–HIRLAM NWP System, *Monthly Weather Review*, 145, 1919–1935, <https://doi.org/10.1175/MWR-D-16-0417.1>, 2017.
- Dee, D. P., Uppala, S. M., Simmons, A. J., et al.: The ERA-Interim reanalysis: configuration and performance of the data assimilation system, *Quarterly Journal of the Royal Meteorological Society*, 137, 553–597, <https://doi.org/10.1002/qj.828>, 2011.
- Ghafarian, P., Pegahfar, N., and Owlad, E.: Multiscale analysis of lake-effect snow over the southwest coast of the Caspian Sea (31 January–5 February 2014), *Weather*, 73, 9–14, <https://doi.org/10.1002/wea.3055>, 2018.
- 420 Hersbach, H., Bell, B., Berrisford, P., et al.: The ERA5 global reanalysis, *Quarterly Journal of the Royal Meteorological Society*, 146, 1999–2049, <https://doi.org/10.1002/qj.3803>, 2020.
- Hjelmfelt, M. R. and Braham, R. R.: Numerical Simulation of the Airflow over Lake Michigan for a Major Lake-Effect Snow Event, *Monthly Weather Review*, 111, 205–219, [https://doi.org/10.1175/1520-0493\(1983\)111<0205:NSOTAO>2.0.CO;2](https://doi.org/10.1175/1520-0493(1983)111<0205:NSOTAO>2.0.CO;2), 1983.
- 425 Holroyd, E. W.: Lake-Effect Cloud Bands as Seen From Weather Satellites, *Journal of the Atmospheric Sciences*, 28, 1165–1170, [https://doi.org/10.1175/1520-0469\(1971\)028<1165:LECBAS>2.0.CO;2](https://doi.org/10.1175/1520-0469(1971)028<1165:LECBAS>2.0.CO;2), 1971.
- Jeworrek, J., Wu, L., Dieterich, C., and Rutgersson, A.: Characteristics of convective snow bands along the Swedish east coast, *Earth System Dynamics*, 8, 163–175, <https://doi.org/10.5194/esd-8-163-2017>, 2017.
- Juga, I.: Sea-effect snowfall – a special hazard for road traffic in the coastal areas of Finland, in: *Proceedings of the 15th SIRWEC Conference*, Quebec City, Canada, 2010.
- 430 Juga, I., Hippi, M., Nurmi, P., and Karsisto, V.: Weather factors triggering the massive car crashes on 3 February 2012 in the Helsinki metropolitan area, in: *Proceedings of the 17th SIRWEC Conference*, La Massana, Andorra, 2014.
- Laird, N. F., Kristovich, D. A. R., and Walsh, J. E.: Idealized Model Simulations Examining the Mesoscale Structure of Winter Lake-Effect Circulations, *Monthly Weather Review*, 131, 206–221, [https://doi.org/10.1175/1520-0493\(2003\)131<0206:IMSETM>2.0.CO;2](https://doi.org/10.1175/1520-0493(2003)131<0206:IMSETM>2.0.CO;2), 2003.
- 435 Lind, P., Belušić, D., Christensen, O. B., Dobler, A., Kjellström, E., Landgren, O., et al.: Benefits and Added Value of Convection-Permitting Climate Modeling over Fenno-Scandinavia, *Climate Dynamics*, 55, 1893–1912, <https://doi.org/10.1007/s00382-020-05359-3>, 2020.
- Lindstedt, D., Lind, P., Kjellström, E., and Jones, C.: A new regional climate model operating at the meso-gamma scale: performance over Europe, *Tellus A: Dynamic Meteorology and Oceanography*, 67, 24 138, <https://doi.org/10.3402/tellusa.v67.24138>, 2015.
- Lucas-Picher, P., Laprise, R., and Winger, K.: Evidence of added value in North American regional climate model hindcast simulations using ever-increasing horizontal resolutions, *Climate Dynamics*, 48, 2611–2633, <https://doi.org/10.1007/s00382-016-3227-z>, 2017.
- 440



- Lucas-Picher, P., Argüeso, D., Brisson, E., Trambay, Y., Berg, P., Lemonsu, A., Kotlarski, S., and Caillaud, C.: Convection-permitting modeling with regional climate models: Latest developments and next steps, *Wiley Interdisciplinary Reviews: Climate Change*, 12, e731, <https://doi.org/10.1002/wcc.731>, 2021.
- Masson, V., Le Moigne, P., Martin, E., Faroux, S., Alias, A., Alkama, R., et al.: The SURFEXv7.2 land and ocean surface platform for coupled  
445 or offline simulation of earth surface variables and fluxes, *Geoscientific Model Development*, 6, 929–960, <https://doi.org/10.5194/gmd-6-929-2013>, 2013.
- Mazon, J., Niemelä, S., Pino, D., Savijärvi, H., and Vihma, T.: Snow bands over the Gulf of Finland in wintertime, *Tellus A: Dynamic Meteorology and Oceanography*, <https://doi.org/10.3402/tellusa.v67.25102>, 2015.
- Médus, E., Thomassen, E. D., Belušić, D., Lind, P., Berg, P., Christensen, J. H., et al.: Characteristics of precipitation extremes  
450 over the Nordic region: added value of convection-permitting modeling, *Natural Hazards and Earth System Sciences*, 22, 693–711, <https://doi.org/10.5194/nhess-22-693-2022>, 2022.
- Niemelä, S.: Winter-time convection - a heavy snowfall case in Southern Finland, *HIRLAM Newsletter*, 59, 21–26, 2012.
- Niziol, T. A.: Operational forecasting of lake effect snowfall in western and central New York, *Weather and Forecasting*, 2, 310–321, [https://doi.org/10.1175/1520-0434\(1987\)002<0310:OFOLES>2.0.CO;2](https://doi.org/10.1175/1520-0434(1987)002<0310:OFOLES>2.0.CO;2), 1987.
- 455 Niziol, T. A., Snyder, W. R., and Waldstreicher, J. S.: Winter Weather Forecasting throughout the Eastern United States. Part IV: Lake Effect Snow, *Weather and Forecasting*, 10, 61–77, 1995.
- Norris, J., Vaughan, G., and Schultz, D. M.: Snowbands over the English Channel and Irish Sea during cold-air outbreaks, *Quarterly Journal of the Royal Meteorological Society*, 139, 1747–1761, <https://doi.org/10.1002/qj.2079>, 2013.
- Notaro, M., Bennington, V., and Vavrus, S.: Dynamically Downscaled Projections of Lake-Effect Snow in the Great Lakes Basin, *Journal of*  
460 *Climate*, 28, 1661–1684, <https://doi.org/10.1175/JCLI-D-14-00467.1>, 2015.
- Olsson, J., Du, Y., An, D., Uvo, C. B., Sörensen, J., Toivonen, E., Belušić, D., and Dobler, A.: An Analysis of (Sub-)Hourly Rainfall in Convection-Permitting Climate Simulations Over Southern Sweden From a User’s Perspective, *Frontiers in Earth Science*, 9, 681 312, <https://doi.org/10.3389/feart.2021.681312>, 2021.
- Olsson, T., Perttula, T., Jylhä, K., and Luomaranta, A.: Intense sea-effect snowfall case on the western coast of Finland, *Advances in Science*  
465 *and Research*, 14, 231–239, <https://doi.org/10.5194/asr-14-231-2017>, 2017.
- Olsson, T., Post, P., Rannat, K., Keernik, H., Perttula, T., Luomaranta, A., et al.: Sea-effect snowfall case in the Baltic Sea region analysed by reanalysis, remote sensing data and convection-permitting mesoscale modelling, *Geophysica*, 53, 65–91, 2018.
- Olsson, T., Luomaranta, A., Jylhä, K., Jeworrek, J., Perttula, T., Dieterich, C., et al.: Statistics of sea-effect snowfall along the Finnish coastline based on regional climate model data, *Advances in Science and Research*, 17, 87–104, <https://doi.org/10.5194/asr-17-87-2020>,  
470 2020.
- Olsson, T., Luomaranta, A., Nyman, H., and Jylhä, K.: Climatology of sea-effect snow in Finland, *International Journal of Climatology*, pp. 1–18, <https://doi.org/10.1002/joc.7801>, 2022.
- Rutgersson, A., Kjellström, E., Haapala, J., Stendel, M., Danilovich, I., Drews, M., Jylhä, K., Kujala, P., Larsén, X. G., Halsnæs, K., Lehtonen, I., Luomaranta, A., Nilsson, E., Olsson, T., Särkkä, J., Tuomi, L., and Wasmund, N.: Natural hazards and extreme events in the Baltic Sea  
475 region, *Earth System Dynamics*, 13, 251–301, <https://doi.org/10.5194/esd-13-251-2022>, 2022.
- Saarikivi, P.: Characteristics of Mesoscale Precipitation Bands in Southern Finland, *Monthly Weather Review*, 117, 2584 – 2593, [https://doi.org/10.1175/1520-0493\(1989\)117<2584:COMPBI>2.0.CO;2](https://doi.org/10.1175/1520-0493(1989)117<2584:COMPBI>2.0.CO;2), 1989.



Steenburgh, W. J. and Nakai, S.: Perspectives on Sea- and Lake-Effect Precipitation from Japan's "Gosetsu Chitai", Bulletin of the American Meteorological Society, 101, E58–E72, <https://doi.org/10.1175/BAMS-D-18-0335.1>, 2020.

480 Swedish Meteorological and Hydrological Institute: Snökanoner från havet, <https://www.smhi.se/kunskapsbanken/meteorologi/sno/snokanoner-fran-havet>, accessed: 15 July 2025, 2025.

Vihma, T. and Haapala, J.: Geophysics of sea ice in the Baltic Sea: A review, Progress in Oceanography, 80, 129–148, <https://doi.org/10.1016/j.pocean.2009.02.002>, 2009.

Westerblom, S.: Projected changes in sea-effect snowfall over the Swedish Baltic Sea region : Results from a high-resolution regional climate  
485 model, 2024.